Science of the Total Environment 587–588 (2017) 36–46

Contents lists available at ScienceDirect

Science of the Total Environment

journal homepage: www.elsevier.com/locate/scitotenv

Effects of weathering on the dispersion of crude oil through oil-mineral aggregation

Sarah A. Gustitus, Gerald F. John, T. Prabhakar Clement *

Environmental Engineering Program, Department of Civil Engineering, Auburn University, Auburn, AL, USA

HIGHLIGHTS

- Different types of artificially weathered oils were used to study OMA formation.
- For all oil types, the amount of oil dispersed as OMA decreases with weathering.
- Reduction in OMA formation is controlled by physical rather than chemical effects.
- After 32 h of weathering, 35% of light and 1% of heavy crude were dispersed.

GRAPHICAL ABSTRACT

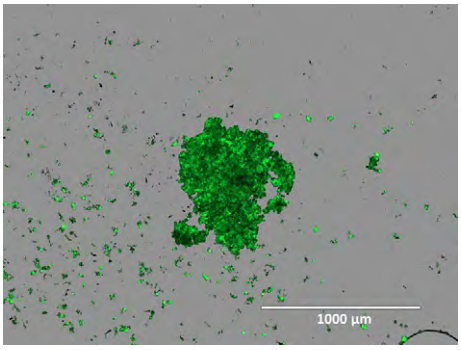

ARTICLE INFO

Article history:
Received 22 November 2016
Received in revised form 16 January 2017
Accepted 5 February 2017
Available online 8 February 2017

Editor: Kevin V. Thomas

Keywords:
Oil-mineral aggregate
Oil spill
Oil weathering
Oil dispersion
Oil-sediment interaction

ABSTRACT

Crude oil that is inadvertently spilled in the marine environment can interact with suspended sediment to form oil-mineral aggregates (OMA). Researchers have identified OMA formation as a natural method of oil dispersion, and have sought ways to enhance this process for oil spill remediation. Currently there is a lack of understanding of how the weathering of oil will affect the formation of OMA due to a lack of published data on this relationship. Based on literature, we identified two conflicting hypotheses: OMA formation 1) increases with weathering as a result of increased asphaltene and polar compound content; or 2) decreases with weathering as a result of increased viscosity. While it is indeed true that the viscosity and the relative amount of polar compounds will increase with weathering, their net effects on OMA formation is unclear. Controlled laboratory experiments were carried out to systematically test these two conflicting hypotheses. Experimental results using light, intermediate, and heavy crude oils, each at five weathering stages, show a decrease in OMA formation as oil weathers.

1. Introduction

When oil is inadvertently spilled in a marine environment, one of the major goals of remediation efforts is to disperse the unrecoverable oil into the water column to enhance various natural degradation processes. Dispersion increases the available surface area of the oil which enhances natural processes such as biodegradation and dissolution that play a significant role in degrading the oil (Prince et al., 2003; Prince et al., 1999). Oil can be naturally dispersed by turbulent currents caused by weather events, such as storms, as was observed following the *Exxon Valdez* oil spill (Wolfe et al., 1994). When weather conditions are insufficient to maintain sustained dispersion, chemical dispersants

* Corresponding author at: 212 Harbert Engineering Center, Auburn University, Auburn, AL 36849, USA.
E-mail address: clement@auburn.edu (T.P. Clement).

http://dx.doi.org/10.1016/j.scitotenv.2017.02.044
0048-9697/

are often used to promote oil dispersion. This approach was used in the aftermath of major oil spill events such as the *Torrey Canyon*, *Deepwater Horizon* and *IXTOC* oil spills (Jernelöv and Lindén, 1981; Kujawinski et al., 2011; Ramseur, 2010). However, there are several concerns about the potential negative toxic effects of chemical dispersants (Chapman et al., 2007; Linden, 1975; Ramachandran et al., 2004), hence it would be desirable to find environmentally friendly alternative dispersion methods to minimize their use until they are proven to be non-toxic.

When spilled oil enters the coastal environment, it can be dispersed naturally by interacting with suspended mineral fines to form small (typically <1 mm) aggregates in the water column (Bragg and Owens, 1995; Fitzpatrick et al., 2015; Lee et al., 1997). In the published literature, these microscopic aggregates are referred to as oil-mineral aggregates (OMA) (Lee et al., 1998). Trapping oil as OMA has been recognized as a method for enhancing oil dispersion, and has long been recognized to play a natural role in the remediation of oiled shorelines (Owens and Lee, 2003). Based on laboratory studies, researchers have postulated that OMA formation must have played a significant role in the natural cleansing of shorelines impacted by the *Exxon Valdez* spill (Bragg and Owens, 1995; Bragg and Yang, 1995). Field studies later confirmed natural OMA formation following the *Sea Empress* spill (Lee et al., 1997).

Over the past two decades, researchers have sought to enhance the formation of OMA in order to augment natural remediation following an oil spill (Fitzpatrick et al., 2015). Enhancing OMA formation as a dispersant technology has several benefits which include cost effectiveness, reduction of oil slicks, and enhanced degradation rates of trapped oil (Sun and Zheng, 2009). OMA formation decreases the amount of oil in the surface slick, and it has also been shown to increase both the rate and the extent of microbial biodegradation of oil in the water column (Lee et al., 1996; Weise et al., 1999). In addition to increasing the availability of the oil to microorganisms, OMA formation could also reduce the bioavailability and toxicity of the oil to aquatic organisms in the affected environment (Fitzpatrick et al., 2015). In order to take advantage of the benefits of dispersion through OMA formation, researchers have sought for years to find ways to better understand and engineer this process as a low-cost remediation technique to manage oil spills.

There are two main methods that have been explored for enhancing OMA formation: 1) relocating oil-contaminated sediment and rocks from high tide to low tide zones to facilitate a remediation process commonly known as "surf washing," and 2) applying fine sediment, usually in the form of a slurry, directly to an oil slick to promote dispersion (Sun and Zheng, 2009). The "surf washing" method has been applied several times to various oiled shorelines. In 1993, oiled sediments in high tide zones following the *Bouchard B-155* oil spill in Tampa Bay, FL were moved into the surf zone by front end loaders, resulting in cleansed sediment after one to two wave cycles (Owens et al., 1995). A similar relocation process was employed following the *Sea Empress* spill in 1996, where most of the beached oil was removed after four days of treatment. The same study verified formation of OMA during the surf washing process using microscopic observations (Lee et al., 1997). A controlled field study that was part of the Svalbard Shoreline Field Trials was carried out using sediment relocation on an experimentally oiled shoreline, where oil-contaminated sediment and rocks were moved from the high tide zone to the low-tide zone. This study confirmed that natural OMA formation can be significantly accelerated by surf washing, leading to a dramatic reduction in the amount of oil trapped on the experimental beach plots (Lee et al., 2003).

In addition to the "surf washing" method, some studies have suggested that oil spill remediation efforts can be enhanced by directly applying fine sediment to an oil slick to facilitate OMA formation (Bragg and Yang, 1995; Lee et al., 2011; Lee et al., 2012). More recent studies have explored various aspects of this idea in greater depth. Zhang et al. (2010) examined the efficiency of OMA formation with alternative materials such as fly ash and graphite that are not typically expected in a beach environment. Additionally, it has been found that modifying the surface properties of minerals such as bentonite or kaolinite can increase OMA formation (Chen et al., 2013; Wang et al., 2011; Zhang et al., 2010). Recently, a mesocosm study was carried out to determine the potential effectiveness of applying a slurry of sediment and water to oil contamination in a reflective beach environment; the study reported that over 21 days an average of a 40% reduction in saturated hydrocarbons was achieved (Silva et al., 2015). Lee et al. (2011) tested the sediment application method in a field study by releasing crude oil into the ice-infested St. Lawrence Estuary. Their team applied a slurry of calcite and seawater directly to the slick and then utilized the propellers of their vessel to create enough mixing energy to form OMA. They found that the oil was quickly dispersed by this treatment, with insignificant resurfacing of the oil. Additionally, mesocosm studies on samples from this field trial showed that over 56% of the spilled oil was degraded after two months, despite the low temperatures.

In order to determine the most effective way to enhance OMA formation, and to predict the natural extent of the aggregation, many studies have been carried out to better understand the fundamentals of the OMA formation process (Gong et al., 2014; Sun and Zheng, 2009). Through these studies, the impacts of several environmental variables including salinity, sediment concentration, temperature, mixing energy, sediment type and oil type have been explored (Gong et al., 2014). In addition to the effects of natural environmental factors, the effect of chemical dispersants on OMA formation has also been thoroughly studied (Cai et al., 2017; Guyomarch et al., 2002; Khelifa et al., 2008; Lee et al., 2012; Li et al., 2007; Wang et al., 2013). However, there is currently a gap in our understanding of how the degree of oil weathering will affect the OMA formation process over time (Sun and Zheng, 2009). Understanding this factor is crucial to extrapolating the results from idealized laboratory experiments, which are typically conducted using fresh oil or a single stage of weathered oil. Quantifying weathering effects on OMA formation will also help improve the capability of mathematical models used to predict the temporal variations in OMA formation, and can help develop guidelines for enhancing OMA formation for the treatment of oil spills. This knowledge can also improve risk assessments for environments where OMA form. For example, Niu et al. (2010) adapted their assessment of the risks of OMA to benthic organisms to account for variations in the chemical composition of weathered oil, but did not adjust the model to account for how the total amount of oil that could be transported to the benthic zone as OMA would change as the oil weathers.

Immediately after a spill, the spilled oil begins to weather at an exponential rate, changing both its chemical and physical properties. First, the viscosity of the oil increases as it weathers, which decreases the ability of the oil to form small droplets (Delvigne and Sweeney, 1988). Additionally, as oil weathers, lighter components (e.g. alkanes, aromatics) are removed, while other heavier components, such as asphaltenes become more concentrated (Oudot et al., 1998). Increases in viscosity and asphaltene content have two major effects on OMA formation: first, oils with higher asphaltene content and viscosity are more likely to form stable emulsions (Bobra, 1991); second, since asphaltenes are amphoteric compounds (Poteau et al., 2005), the increase in asphaltene content due to the concentration effect (Trudel et al., 2010) will make weathered oil increasingly attracted to charged surfaces such as clay particles (Bragg and Yang, 1995; Guyomarch et al., 2002).

Most OMA studies use only fresh oil, or a single weathered stage of an oil, and as a result there are some disagreements in the published literature about whether OMA formation increases or decreases as a result of weathering. Based on literature, we have identified two conflicting research hypotheses. We first hypothesize that increased relative quantities of polar and charged hydrocarbons, such as asphaltenes, found in weathered oil will cause an increase in dispersion through OMA formation by increasing the attractive forces between the oil and the negatively charged mineral surface (Bragg and Yang, 1995; Sørensen et al., 2014; Stoffyn-Egli and Lee, 2002). Bragg and Yang (1995) found that

weathered oil from the Exxon Valdez spill formed small OMA more readily than a degassed Alaska North Slope oil with low polar content which had a similar viscosity; they used this data to suggest that OMA would form more readily with weathered oil. More recently, Sørensen et al. (2014) tested between four different oils and found that those with significantly greater asphaltene content had a greater propensity to adsorb to suspended particulate matter, and therefore predicted that as crude oil weathered and increased in polar content, its ability to form OMA would increase. Our second hypothesis is that the increased viscosity of weathered oils will decrease the formation of OMA. Payne et al. (2003) postulated that increased viscosity associated with oil weathering will lead to diminished oil droplet dispersion and thus decrease OMA formation over time, although their specific experimental conditions prevented direct observations to support this hypothesis. This hypothesis is supported in part by other studies that compared different types of oils with varying viscosities, which have shown that higher viscosity oils form fewer OMA (Kepkay et al., 2002; Khelifa et al., 2002).

Interestingly, the first hypothesis predicts an increase in OMA formation with weathering, while the second predicts a decrease. The objective of this study is to test these two conflicting hypotheses and quantify how the degree of weathering will affect the amount of oil that can be dispersed as OMA. Of the published OMA studies that have used either artificially or naturally weathered oil (Khelifa et al., 2002; Li et al., 2007; Ma et al., 2008; Omotoso et al., 2002; Payne et al., 2003; Wang et al., 2013), very few have compared OMA formation using weathered oil to OMA formed from that oil's fresh counterpart, and none of these studies have examined multiple stages of weathering for the same oil. In this study, five stages of weathering are examined for three types of oil to evaluate how oil dispersion through OMA formation will change as weathering progresses. The results will serve two major purposes: 1) determine if OMA formation increases or decreases with weathering; and 2) determine, through microscopic analyses, how OMA structure will change with weathering.

2. Methods

2.1. Materials

Three types of oil were used in this study: Louisiana Sweet Crude (LSC), Texas Intermediate Crude (TIC), and California Heavy Crude (CHC). LSC oil was supplied by Goodway Refining LLC (Atmore, AL, USA). TIC oil was supplied by Texas Raw Crude (Midland, TX, USA). CHC oil was supplied by ExxonMobil Corporation (Benicia, CA, USA).

All experiments were performed using kaolinite, which has been identified as one of the most effective natural minerals for formation of OMA (Poirier and Thiel, 1941; Wang et al., 2011; Zhang et al., 2010). Natural kaolinite was purchased from Sigma-Aldrich (St. Louis, MO). Dichloromethane (DCM), sodium chloride (NaCl), and cellulose filter papers were supplied by VWR Scientific (Suwannee, GA).

2.1.1. Oil weathering

Each type of oil was weathered for 2, 4, 8, and 32 h, and these stages will be referred to as W2h, W4h, W8h and W32h, respectively; fresh oil will be referred to as W0h. Oil weathering was simulated by dispensing oil onto glass dishes in thin layers (<1 cm thick) and placing these dishes outside in direct sunlight (Fig. 1). The dishes were left stationary other than to periodically redistribute the oil by shaking to ensure even weathering. In order to prevent debris from contaminating the oil, the dishes were placed in shallow boxes covered with glass panels. The sides of the boxes were screened to allow for ventilation, but to prevent debris from entering the box. When the samples were not outside, they were stored in a freezer at −15 °C. The amount of solar radiation that the oil was exposed to while weathering was tracked using data from the local weather station located in Auburn, AL. The outdoor weathering method used was similar to the approach used in one of our previous studies (John et al., 2016).

Based on our experimental design, the outdoor weathered oil underwent both evaporation and photodegradation, two major weathering processes experienced by oil slicks. Our previous research has shown that the glass plate used for covering the protective box (Fig. 1) had a negligible effect on evaporation and photodegradation (John et al., 2016).

2.1.2. Mass loss of oil

The percent mass loss of each stage of weathered oil was determined by comparing the weight of the plate with the fresh oil on it to the weight of the plate with the weathered oil on it.

2.1.3. Viscosity of oil

The viscosity of the fresh and weathered oils was determined using a Brookfield rotational viscometer. All stages of LSC, and TIC-W0h were analyzed using spindle 21 and a small sample adapter. The remaining weathering stages of TIC, and all stages of CHC were analyzed using spindle 7.

2.1.4. Asphaltene content of oil

Asphaltene content was determined following a modified method of ASTM D3279-12. Fresh oil (10 g for LSC, 0.5 g for TIC, and 0.1 g for CHC) was carefully weighed into a 250 mL Erlenmeyer flask. Approximately 100 mL of n-hexane was added. The contents were stirred and heated at 40 °C for 20 min and then filtered through a cleaned glass fiber filter. The glass fiber filter was then dried at 105 °C for 2 h and then weighed to determine the asphaltene content in the oils.

Since asphaltenes are conservative compounds and are resistant to weathering (Oudot et al., 1998), the asphaltene content of the weathered oils was estimated based on percent mass loss of oil after weathering using the following formula,

$$ac_f = \frac{ac_o}{(1 - m_{loss})} \quad (1)$$

Fig. 1. Experimental methods: Left) outdoor oil weathering method; Right) baffled flask experiments.

where ac_o is the original asphaltene content measured in the lab, ac_f is the final estimated asphaltene content at a given weathering stage, and m_{loss} is the percent mass loss of the oil due to weathering.

2.1.5. Mineral characterization

The kaolinite was characterized using a Malvern Mastersizer 3000. D_{50} for the kaolinite was 8.2 μm.

2.1.6. Artificial seawater

Artificial seawater (ASW) was produced by dissolving NaCl in deionized water at 3.3 wt% (Sun et al., 2014).

2.2. Experimental procedure

2.2.1. OMA formation

Experiments were performed following a modified version of the baffled flask test (Venosa and Holder, 2013; Venosa et al., 2002). While commonly used for experiments with chemical dispersants, baffled flasks have also been used previously for OMA experiments (Lee et al., 2012; Ma et al., 2008; Zhang et al., 2010). Based on preliminary experiments, four replicates of each experiment were performed to measure the total concentration of oil trapped in OMA; a separate replicate was performed and analyzed on a microscope to quantify the size of oil droplets incorporated in the OMA as well as to characterize the different types of OMA formed (Stoffyn-Egli and Lee, 2002).

Three oils were examined (LSC, TIC, and CHC), each at five stages of weathering (W0h, W2h, W4h, W8h and W32h). Each of the weathering stages was tested at a low (100 mg/L) and high (200 mg/L) suspended sediment content (Sun et al., 2010). Experimental conditions are summarized in Table 1.

Each experiment was done using a baffled flask (VWR Scientific) fitted with a stopcock near the bottom. First, either 12 mg or 24 mg of kaolinite was added dry to the flask for low and high sediment concentration experiments, respectively. The flask was then filled with 120 mL of artificial seawater, sealed with a rubber stopper and mixed on an orbital shaker at 250 rpm for ten minutes to suspend the kaolinite (Wang et al., 2011; Zhang et al., 2010). Next, 24 mg of oil was dispensed directly onto the water surface using a syringe. The weight of oil applied was measured by weighing the syringe before and after the oil was dispensed. The flask containing oil, artificial seawater, and kaolinite was then covered and shaken at 250 rpm on the orbital shaker for 1 h, after which OMA formation is assumed to have leveled off at this shaking rate (Sun et al., 2014). Flasks were removed from the shaker and allowed to settle overnight for a minimum of 8 h, after which negatively buoyant OMA, the dominant form following the settling period, were separated for extraction (Khelifa et al., 2008; Sun et al., 2014; Sun et al., 2010). A vacuum pump was used to remove the topmost portion of the flask, leaving behind approximately 20 mL of artificial seawater and negatively buoyant OMAs in the flask (Khelifa et al., 2008). The remaining contents of the flask were transferred directly to a separatory funnel for extraction.

Table 1
Experimental conditions.

Parameter	Type/value
Artificial seawater volume	120 mL
Types of oil used	Louisiana Sweet Crude (LSC) Texas Intermediate Crude (TIC) California Heavy Crude (CHC)
Oil concentration (amount added)	200 mg/L (24 mg)
Weathering stages	Fresh; weathered for 2, 4, 8 and 32 h
Sediment	Kaolinite
Sediment concentration (amount added)	100 mg/L (12 mg) 200 mg/L (24 mg)
Shaking time	1 h
Shaking rate	250 rpm
Settling time	>8 h

2.2.2. Extraction

Extraction was done following a modified version of the extraction protocol outlined by Khelifa et al. (2008). The remaining suspension of kaolinite and OMA was transferred to a 50 mL separatory funnel. DCM was added for each of three consecutive extractions so that the DCM to water ratio was 1:2 for the first extraction, and 1:5 for each of two additional extractions. The extracts were combined and run through a Whatman cellulose filter with a pore size of 0.45 μm. The filtered extract was blown down under a gentle stream of nitrogen gas, reconstituted to a total volume of 10 mL with DCM, and stored at 4 °C until analysis.

2.2.3. Analysis — quantifying oil trapping efficiency using spectrophotometry

The concentration of oil captured in the negatively buoyant OMA was determined through analysis with a SpectraMax M2 spectrophotometer (Molecular Devices) using a modified version of the method outlined in Venosa and Holder (2013). Calibration standards were produced by adding a known quantity of oil (25, 50, 125, 250, 375, and 625 mg) to a vial containing approximately 22 mL ASW and approximately 24 mg kaolinite, and then extracting this suspension using the same procedure outlined in Section 2.2.2. The calibration standards and experimental extracts were analyzed on the spectrophotometer at wavelengths of 340, 370 and 400 nm. Extracts which were too concentrated to be read on the instrument were diluted as needed, and the formulas were corrected for the dilution.

The area under the absorbance vs. wavelength curve between 340 and 400 nm was determined using the trapezoidal rule with Eq. (2):

$$Area = \frac{(Abs_{340} + Abs_{370}) \times 30}{2} + \frac{(Abs_{370} + Abs_{400}) \times 30}{2} \quad (2)$$

The response data for the calibration standards were used to generate a calibration curve, which was then used to determine the concentration of extracts from experiments. Oil trapping efficiency was determined using the following formulas:

$$mass_{OMA} = \frac{Area - b}{m} \times V_{extract} \quad (3)$$

where $mass_{OMA}$ is the mass of oil in the negatively buoyant OMA, m and b are the y-intercept and slope of the calibration curve respectively, and $V_{extract}$ is the volume of the extract, and

$$OTE(\%) = \frac{mass_{OMA}}{mass_{oil}} \quad (4)$$

where OTE is the oil trapping efficiency, which is the ratio of the mass of oil trapped in OMA ($mass_{OMA}$) to the total mass of oil originally introduced in the experiment ($mass_{oil}$).

2.2.4. Analysis — UV-epifluorescence microscopy

One replicate of each experiment was used to analyze the structure of the OMA formed based on the structures identified in Stoffyn-Egli and Lee (2002) (i.e. single droplet, multiple droplet, solid, and flake OMA), including the size of oil droplets incorporated in the OMA. These replicates were run separately from the replicates analyzed for total oil concentration; therefore, an additional replicate was performed, extracted and measured with this set to ensure that results were consistent between trials. The suspension of negatively buoyant OMAs from each microscopy replicate was brought to a total volume of 22 mL with ASW; 10 μL of this suspension was dispensed onto a glass slide. The wet mount was analyzed using a microscope (Advanced Microscopic Group AMAFD1000) with both fluorescent and brightfield microscopy modes. Using fluorescence only, images of 30–40 consecutive fields of view were taken of each slide (Sun et al., 2014). These images were analyzed using ImageJ software (NIH) to measure oil droplet diameter (Rasband, 2016). OMA structures were identified by generating an

overlay of the fluorescent image and the transmitted light image so that both oil and sediment could be observed in the same field of view.

2.3. Data analysis

The oil trapping efficiency data was statistically analyzed using Welch's *t*-test and Pearson correlation. The statistical analysis was done using RStudio (R version 3.2.2).

3. Results

3.1. Oil properties

3.1.1. Fresh oils

The three oils used in this study were selected for their range of oil types, fresh viscosity values and asphaltene contents. LSC had the lowest viscosity and asphaltene content, followed by TIC, and CHC had the highest viscosity and asphaltene content (Fig. 2).

3.1.2. Weathered oils

The viscosity, asphaltene content, and percent mass loss were measured for each stage of weathered oil. Solar radiation was tracked to ensure that samples which were not weathered simultaneously were exposed to comparable levels of solar radiation. The solar radiation exposure, viscosity, asphaltene content and mass loss for each weathering stage of oil are shown in Fig. 2. The asphaltene content for the weathered oils was estimated from measurements done with fresh oils and the percent mass loss. This is due to the formation of polar constituents during the weathering process which are insoluble in hexane and therefore cause an overestimation of asphaltene content (Oudot et al., 1998). The high resistance of asphaltenes to evaporation and photodegradation for the given exposure time, makes this a reasonable estimation.

3.2. Oil trapping efficiency

The overall capability of an oil to form OMA was quantified as an oil trapping efficiency, which was derived from the spectrophotometric data by computing the fraction of total oil trapped as negatively buoyant OMA with reference to the total amount of oil originally introduced into the system. The oil trapping efficiencies for LSC, TIC and CHC as they weathered over time are summarized in Fig. 3.

For LSC, the oil trapping efficiency decreases as the oil weathers. The oil trapping efficiency at the low sediment concentration is significantly lower (Welch *t*-test, $p < 0.05$) than at the high sediment concentration for all weathering stages except for LSC-W32h for which the efficiency is statistically similar ($p > 0.05$) between low and high sediment concentration experiments. The more efficient trapping for the higher sediment concentration agrees with the previous findings reported by other studies (Ajijolaiya et al., 2006; Khelifa et al., 2007; Khelifa et al., 2008; Sun et al., 2010). The oil trapping efficiency for low and high sediment concentration, respectively, decreases from 71% and 81% for LSC-W0h, to 29% and 35% for LSC-W32h. Preliminary experiments with sediment concentrations higher than 200 mg/L were conducted, and the oil trapping efficiency was not significantly higher ($p < 0.05$) than experiments performed with a sediment concentration of 200 mg/L.

Similar to LSC, for TIC the oil trapping efficiency decreases as the oil weathers and is significantly lower for the low sediment concentration for all weathering stages except for TIC-W32h, for which the oil trapping efficiency at the two sediment concentrations is statistically similar. The oil trapping efficiency for low and high sediment concentration,

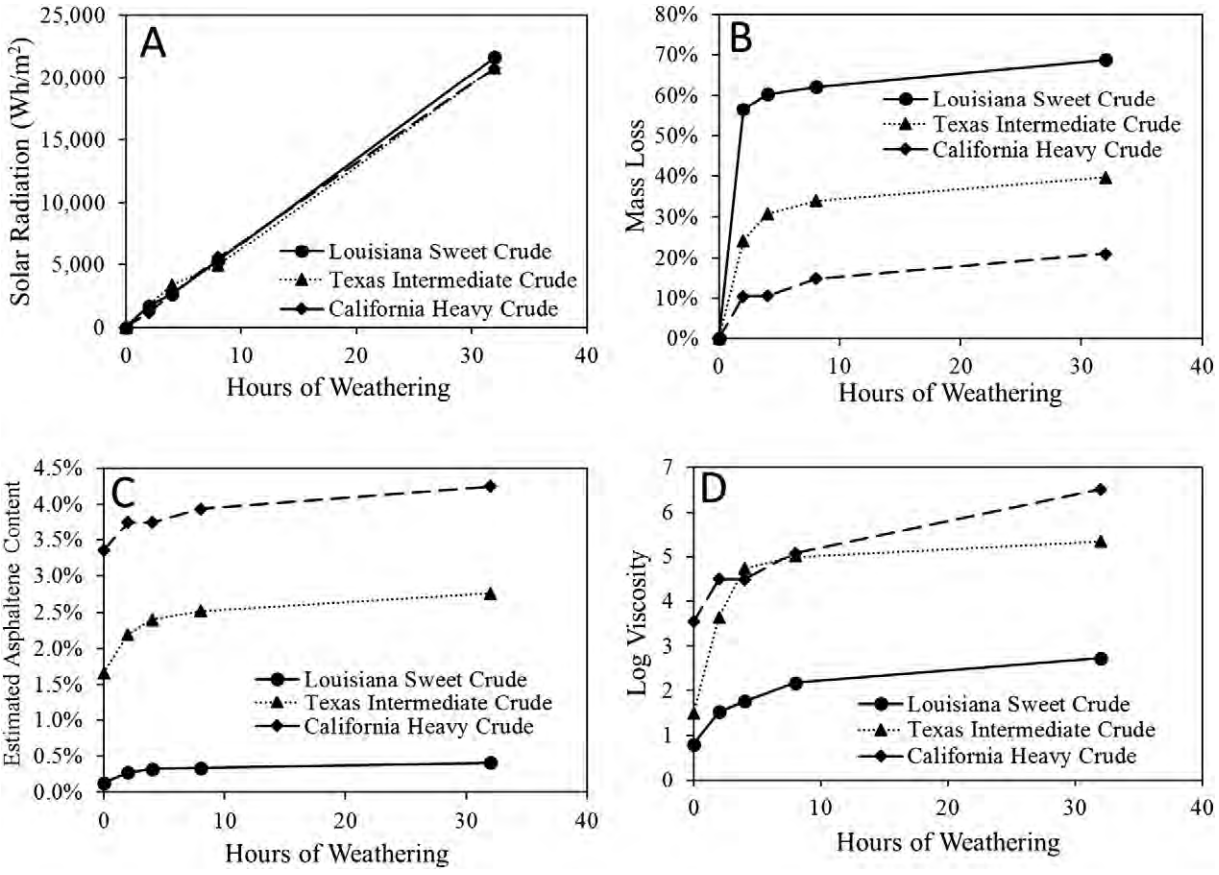

Fig. 2. A) Cumulative amount of solar radiation; B) percent mass loss due to weathering; C) increases in asphaltene content due to weathering; and D) increases in viscosity (in log scale) due to weathering.

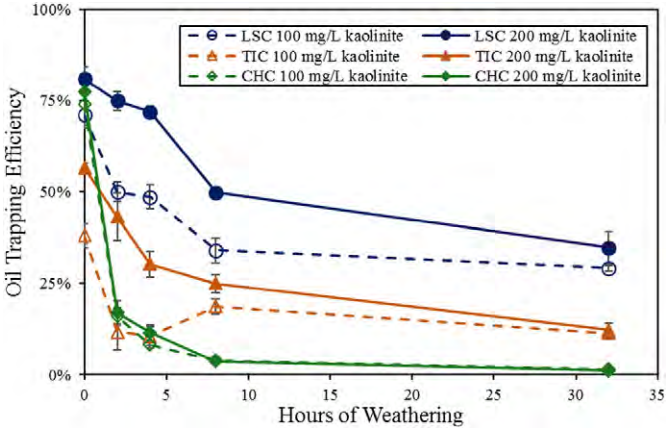

Fig. 3. Oil trapping efficiency at various weathering levels for Louisiana Sweet Crude (LSC), Texas Intermediate Crude (TIC), and California Heavy Crude (CHC). Open symbols with dotted lines indicate values at low sediment concentrations and filled symbols with continuous lines indicate values at high sediment concentrations.

respectively, decreases from 38% and 57% for TIC-W0h, to 11% and 12% for TIC-W32h.

For CHC, the oil trapping efficiency is statistically similar for low and high sediment concentration experiments at all weathering stages except for CHC-W4h, for which the trapping efficiency is significantly lower for the low sediment concentration. The oil trapping efficiency for low and high sediment concentration, respectively, decreases from 77% and 74% for CHC-W0h, to 1% at both sediment concentrations for CHC-W32h.

The correlations of oil trapping efficiency with asphaltene content and oil trapping efficiency with viscosity were tested using Pearson's correlation. The oil trapping efficiency for all three oils has a high negative correlation (>0.75) with asphaltene content. The correlation of oil trapping efficiency with viscosity decreases as the original viscosity of the oil increases. For LSC, the lightest of the oils, oil trapping efficiency and viscosity have a high negative correlation (0.76); for TIC, the intermediate oil, there is a slightly lower correlation (0.61); and for CHC, the heaviest of the oils, oil trapping efficiency and viscosity have the lowest correlation (0.38).

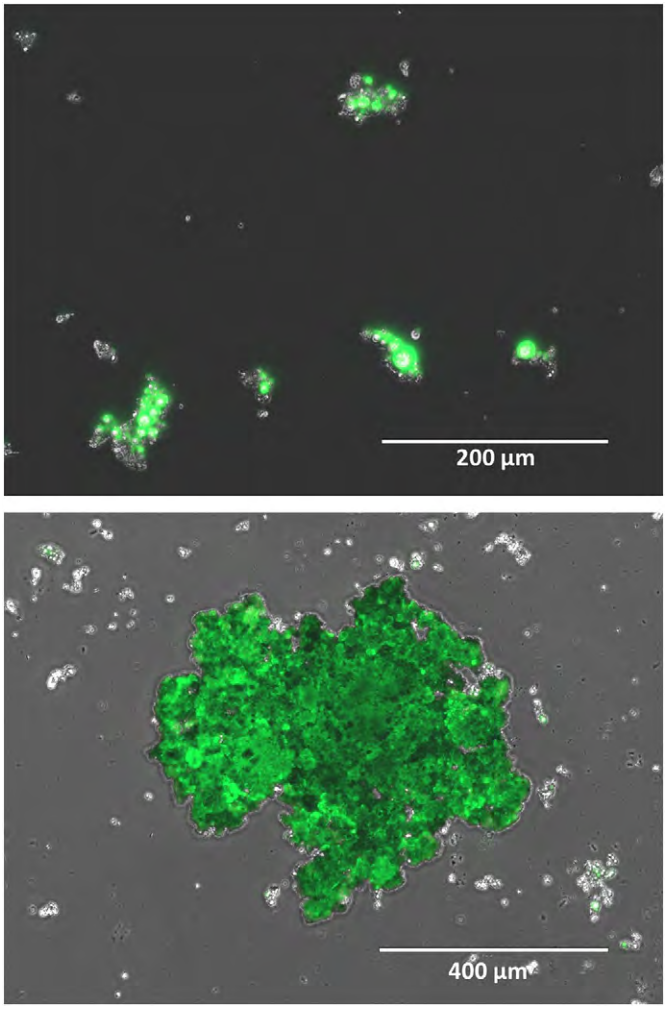

Fig. 4. Top) Image taken at 20× magnification showing single and multiple droplet OMA with droplets ranging in size from 1 to 20 µm formed from fresh Louisiana Sweet Crude; Bottom) image taken at 10× magnification showing a large solid OMA (≈500 µm), as well some small droplet OMA which were formed with 32-hour weathered Louisiana Sweet Crude.

3.3. OMA structure

3.3.1. OMA morphology

Observed OMA were classified based on the types of OMA identified by Stoffyn-Egli and Lee (2002). Single droplet OMA consist of a single spherical droplet of oil surrounded by sediment particles; multiple droplet OMA contain several spherical oil droplets stabilized by sediment particles; and solid OMA are irregularly shaped aggregations of oil and mineral particles where individual droplets are not distinguishable. Flake OMA, which appear as membranes, were not observed in any of the experiments in this study.

Single droplet and multiple droplet OMA made up the entirety of LSC-W0h, LSC-W2h, and LSC-W4h OMA observed (Fig. 4a), and were the numerically predominant form of OMA formed from LSC-W8h and LSC-W32h oils. A small number of the OMA formed from LSC-W8h and LSC-W32h were in the form of solid OMA (Fig. 4b). Solid OMA have previously been found on the scale of tens of microns, sometimes reaching up to 300 µm (Gong et al., 2014; Stoffyn-Egli and Lee, 2002). The observed solid OMA formed from LSC-W8h oil typically fell in this range; however, solid OMA formed from LSC-W32h oil were found that approached 1 mm in length, more than triple the size of previously observed solid OMA. These large solid OMA approach the upper limit of the size of aggregates that are commonly referred to as OMA (Fitzpatrick et al., 2015).

Only single and multiple droplet OMA were observed to have been formed for all stages of TIC (Fig. 5). The droplets incorporated into these OMA tended to be relatively uniform in size, with diameters typically ranging from 1 to 20 µm throughout all weathering stages. A small number of larger droplets were found with diameters up to 85 µm.

The vast majority of OMA formed from CHC were single droplet OMA; multiple droplet OMA were also present, albeit far less common. Extremely large single droplet OMA (100–500 µm diameter), which were visible to the naked eye, were also present in OMA formed with all stages of the oil (Fig. 6). These extremely large droplets are likely a result of the high viscosity of CHC throughout all weathering stages.

3.3.2. Droplet size distribution

The size distributions of droplets in OMA formed from each oil are shown in Fig. 7. The figure shows the percent droplet size smaller than the corresponding values indicated on the x-axis. The average droplet sizes and the droplet size ranges measured in droplet OMA for different oils are summarized in Table 2. The diameter of droplets incorporated into single or multiple droplet OMA was measured for all oil types and weathering stages. Only oil droplets that could be distinctly identified as an individual droplet were measured; therefore, a large

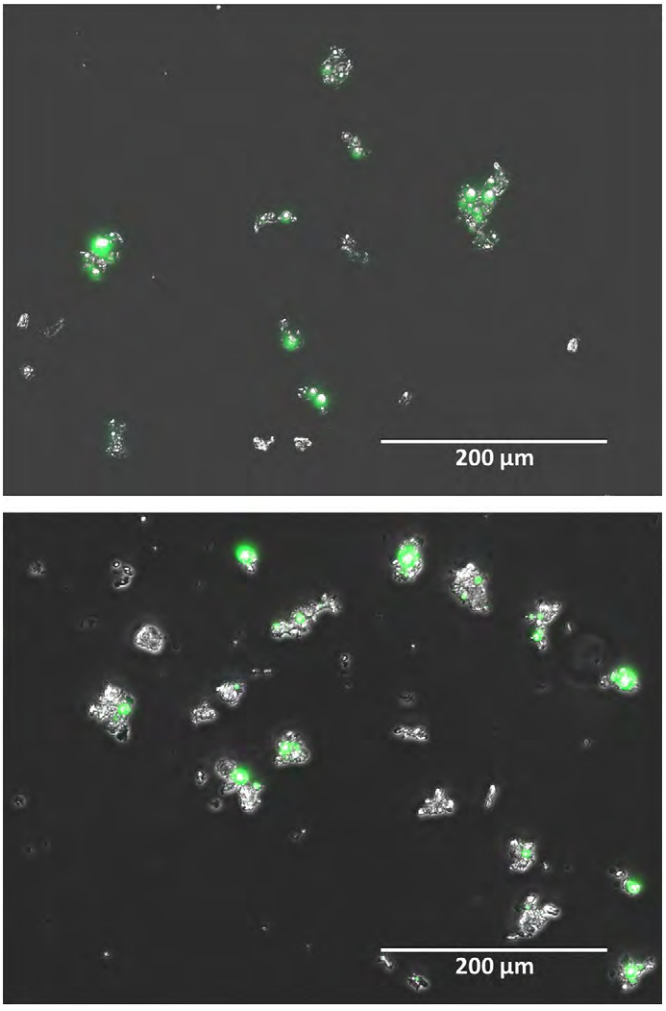

Fig. 5. Top) Image showing single and multiple droplet OMA with droplets ranging in size from 1 to 20 µm formed with fresh Texas Intermediate Crude; Bottom) image showing single and multiple droplet OMAs formed with 32-hour weathered Texas Intermediate Crude. Both images were taken at 20× magnification.

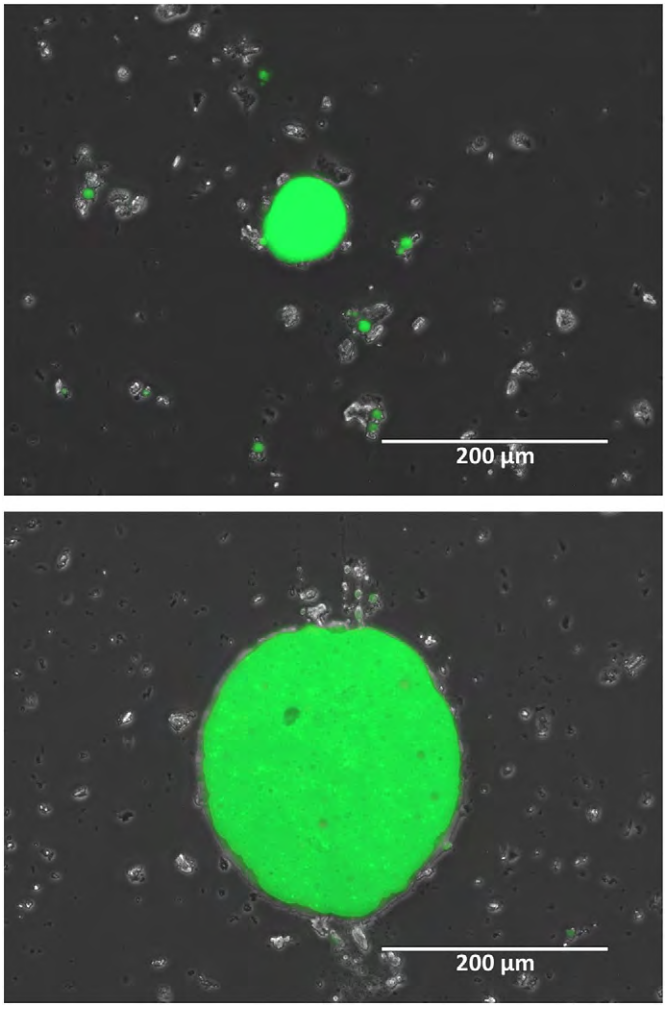

Fig. 6. Top) Image showing single droplet OMA with droplets ranging in size from 10 to 50 µm formed from fresh California Heavy Crude; Bottom) image showing a large single droplet OMA with a droplet approximately 250 µm in diameter formed from 32-hour California Heavy Crude. Both images were taken at 20× magnification.

amount of droplets incorporated into multiple droplet OMA were not quantified.

For LSC, the size of droplets incorporated in OMA increased with weathering. For example, in high sediment concentration experiments the observed droplet size ranged from 1.2 to 28.8 µm for LSC-W0h and from 1.6 to 37.9 µm for LSC-W32H. The average droplet size was 5 ± 3 µm (622 droplets counted) and 9 ± 4 µm (1181 droplets counted) at high sediment concentration for LSC-W0h and LSC-W32h respectively. Both the average and the maximum observed droplet size increased from LSC-W0h to LSC-W32h (Table 3).

For TIC, the size of oil droplets incorporated in OMA decreased with weathering. For example, in low sediment concentration experiments the observed droplet size ranged from 1.8 to 34.2 µm for TIC-W0h and from 1.5 to 31.3 µm for TIC-W32h. The average droplet size was 8 ± 5 µm (464 droplets counted) and 5 ± 4 µm (426 droplets counted) at low sediment concentration for TIC-W0h and TIC-W32h, respectively. The average droplet size decreased from TIC-W0h to TIC-W32h samples. There was no clear trend in the maximum droplet size observed from TIC-W0h to TIC-W32h.

Similar to TIC, the droplet size of CHC oil incorporated in OMA decreased with weathering. For low sediment concentration experiments with CHC, the observed droplet size ranged from 0.9 to 90.5 µm for CHC-W0h and from 0.6 to 147.4 µm for CHC-W32h. The average droplet size was 5 ± 8 µm (306 droplets counted) and 2 ± 6 µm (531 droplets counted) at low sediment concentration for CHC-W0h and CHC-W32h, respectively. The average droplet size decreased from CHC-W0h to CHC-W32h samples, while the maximum droplet size observed increased. However, it should be noted that the variabilities in the average values are extremely high due to some outliers.

4. Discussion

4.1. Effect of weathering on OMA formation

Weathering of crude oil in the natural environment greatly alters the oil's chemical composition. As oil weathers, the lighter compounds leave the system, and the concentration of heavier compounds, including asphaltenes, increases due to the concentration effect (Fig. 2c). Asphaltenes are charged molecules, therefore as their concentration increases in the weathered oil, the oil's ability to attract clay particles increases. Additionally, when oil undergoes photodegradation a wide variety of daughter products are produced, including polar compounds, which should further increase the attraction of the oil to charged surfaces such as clay particles. Increased polar fractions and asphaltene content may help facilitate the OMA formation process to some degree, however, the clear decrease in oil trapping efficiency as each of the three oils weathered disproves our first hypothesis that OMA formation will increase as oil weathers due to an increased charge in the oil. Contrary

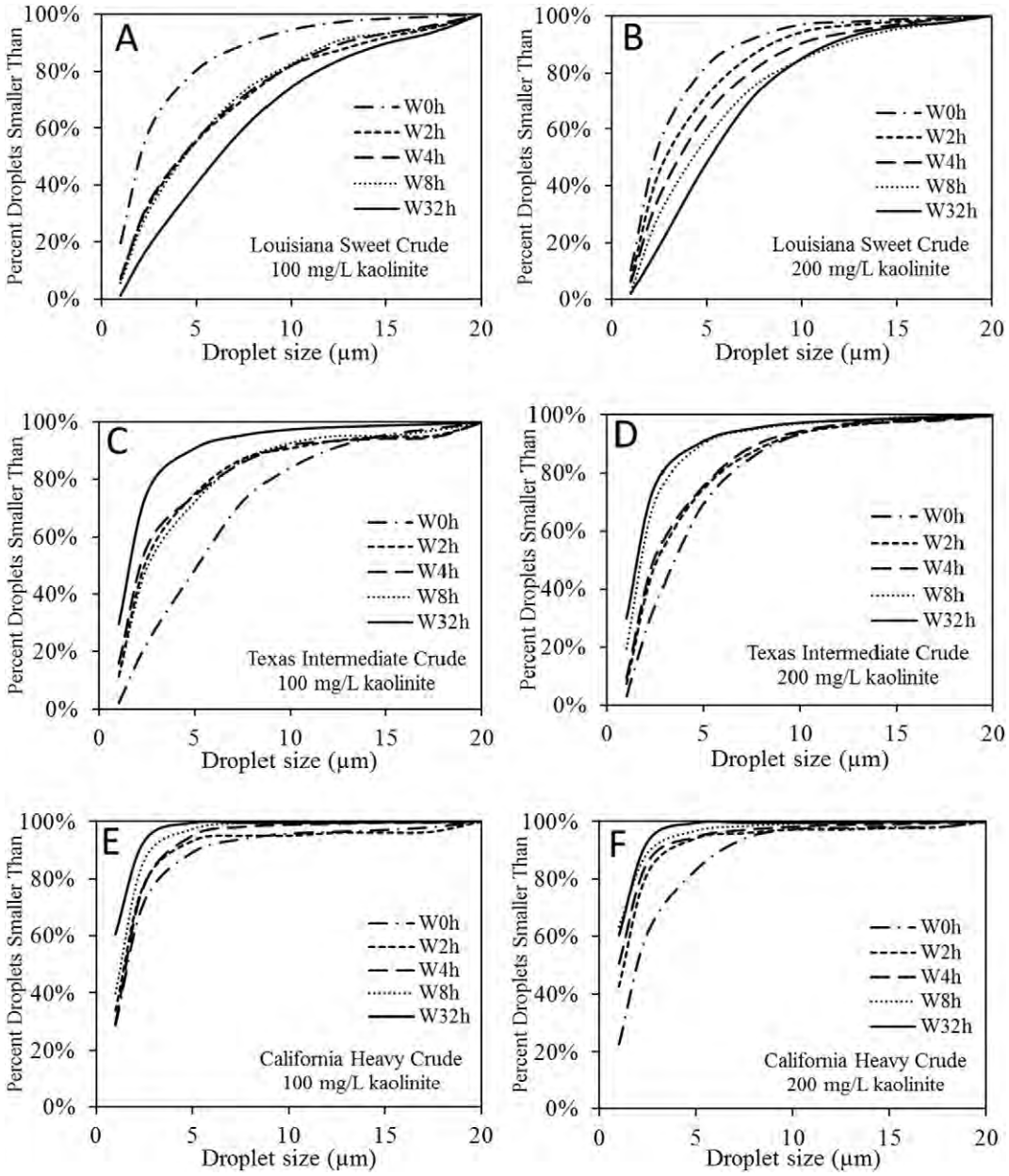

Fig. 7. Cumulative size distribution of droplets incorporated into single and multiple droplet OMA formed from Louisiana Sweet Crude at low (A) and high (B) sediment concentrations; Texas Intermediate Crude at low (C) and high (D) sediment concentrations; and California Heavy Crude at low (E) and high (F) sediment concentrations.

to the suggestions of other studies (Bragg and Yang, 1995; Sørensen et al., 2014; Stoffyn-Egli and Lee, 2002), our study shows no evidence that increased ratios of polar and charged components in oil will overcome the detrimental effects that other weathering-induced physical and chemical changes will have on OMA formation. Lower molecular weight polar compounds which are water-soluble (Lee, 2003) may leave the spilled oil system due to their higher solubility, which might explain, in part, why the polar fraction does not play a more significant role in enhancing OMA formation.

The physical properties of oil are also altered through weathering; most notably the viscosity of oil increased significantly as it weathered (Fig. 2d). The results of this study indicate that the amount of oil that can be dispersed as OMA is highest immediately following a spill, when the oil is still fresh and has the lowest viscosity. At later times, the amount of oil incorporated into OMA will continuously decline as the oil is exposed to the environment. These results support our hypothesis that the increased viscosity of weathered oils will decrease the oil's ability to disperse through formation of OMA. This is consistent with the suggestion of Payne et al. (2003) that drastic increases in viscosity due to weathering will cause OMA formation to diminish in the days following a spill.

The results of this study show that despite increases in polar and charged compounds, the drastic increase in viscosity over time results in a net decrease in dispersion through OMA formation as oil weathers. Payne et al. (2003) suggested that increased weathering would cause OMA formation to be limited to 24–48 h after a spill, except in cases of extremely high turbidity from severe storms or large waves in the nearshore environment. However, the relatively successful trapping efficiency of LSC-W32h, which is representative of a light crude oil weathered for approximately four sunny days (8 h of intense sunlight per day) suggests that for lighter oils, OMA formation may continue for a more extended period of time following a spill. This was not the case with TIC or CHC, which had oil trapping efficiencies of only around 10% and 1% respectively for W32h oil; therefore, after several days of

Table 2
Droplet sizes observed in oil mineral aggregates formed with Louisiana Sweet Crude (LSC), Texas Intermediate Crude (TIC) and California Heavy Crude (CHC) oils. W0h represents fresh oil, and W2h, W4h, W8h and W32h represent oil that is weathered for 2, 4, 8 and 32 h, respectively.

	Droplet size (μm)																			
	W0h				W2h				W4h				W8h				W32h			
	Sediment content				Sediment content				Sediment content				Sediment content				Sediment content			
	Low		High		Low		High		Low		High		Low		High		Low		High	
Oil	Mean	Range	Mean	Range	Mean	Range	Mean	Range	Mean	Range	Mean	Range	Mean	Range	Mean	Range	Mean	Range	Mean	Range
LSC	5 ± 4	0.65–43.44	5 ± 3	1.19–28.83	8 ± 6	0.91–54.10	6 ± 4	1.21–32.45	8 ± 5	0.97–40.02	7 ± 4	1.22–29.52	8 ± 5	0.65–45.11	8 ± 5	1.72–44.28	10 ± 6	1.93–63.07	9 ± 4	1.63–37.92
TIC	8 ± 5	1.77–34.16	7 ± 3	1.40–26.31	7 ± 7	1.16–56.31	6 ± 4	1.21–31.99	7 ± 9	1.29–85.24	6 ± 5	1.29–69.60	6 ± 5	1.61–42.76	5 ± 4	1.05–76.46	5 ± 4	1.46–31.25	4 ± 3	0.73–36.38
CHC	5 ± 8	0.86–90.5	5 ± 6	0.93–79.12	5 ± 8	0.82–86.40	4 ± 7	0.57–107.08	4 ± 5	0.85–69.13	4 ± 7	0.64–150.86	4 ± 7	0.86–125.49	3 ± 2	0.76–26.63	2 ± 6	0.64–147.43	3 ± 12	0.81–227.84

weathering, dispersion through OMA formation should be considered to have minimal impact on spills of these heavier oils.

4.2. Effects of weathering OMA structure

The decreasing ability of an oil to disperse as small droplets as viscosity increases is a well understood concept (Delvigne and Sweeney, 1988). As oil weathers, the viscosity increases, leading to the formation of larger droplets. This trend is evident in observations of LSC oil droplets trapped in OMA (Fig. 7a and b). These larger droplets result in a decrease in surface area, and therefore a decrease in interactions between clay and oil resulting in reduced oil trapping efficiency.

Observations of TIC and CHC oil droplets in OMA demonstrates a trend contrary to that shown for LSC. For both TIC and CHC, the size of observed droplets decreases with increased weathering (Fig. 7c, d, e and f). Sun et al. (2014) suggested that suspended particulate matter may decrease the diameter of dispersed oil droplets. These results indicate that this may be increasingly true for more weathered stages of intermediate and heavy crude oils.

5. Implications

This study demonstrates that OMA formation will decrease as crude oil weathers, irrespective of the original viscosity and asphaltene content for the types of oil examined here. Since the open ocean typically has very little suspended particulate matter, natural OMA formation should have little to no effect on the dispersion of the oil while it remains far from the shore. Therefore, the proximity of a spill to the shoreline, and consequently the amount of time that an oil can weather as it is transported, can have a drastic effect on how the oil is naturally dispersed through OMA formation. Results from LSC show that for a light crude oil, significant amounts of oil can be dispersed as OMA, even days after a spill; however, results from TIC and CHC indicate that the amount of oil that can be dispersed as OMA will be significantly limited for intermediate and heavy crude oils after only a day or two of weathering, compared to dispersion when they are fresh. While dispersing oil through facilitating OMA formation may not be more effective than using chemical dispersants in environments that are favorable to oil weathering, it could be the only prudent alternative when the use of chemical dispersants is undesirable or prohibited, such when an oil spill affects a highly sensitive coastal environment that supports diverse flora and fauna.

Microscopic analysis showed that weathering altered the type of OMA formed only for LSC. Otherwise, the type of OMA formed and the size of the droplets incorporated in OMA stayed relatively consistent throughout the weathering stages; only the total amount of dispersed oil differed. This could have implications on the bioavailability of the oil that is captured within OMA. Based on available surface area alone, the bioavailability for TIC and CHC would not be expected to change significantly, although the bioavailability of LSC trapped in OMA might decrease with weathering as solid OMA become more dominant. However, the composition of the weathered oil differs from that of fresh oil, which will also inevitably affect the degradation of the oil (Clement et al., 2017; Yin et al., 2015). Further studies are needed to quantify the degree to which the various degradation processes differ for OMA formed from oil at various stages of weathering.

Field trials are needed to gain a more comprehensive understanding of how weathering affects OMA formation as a result of weathering processes such as emulsification, dissolution and biodegradation (which were not simulated in this study), and additional external environmental parameters (e.g. sunny vs cloudy, or hot vs cold). Better understanding of these environmental effects could help develop improved mathematical models for predicting natural OMA formation, as well as useful guidelines for promoting engineered enhancement of OMA formation as an oil spill remediation method.

Acknowledgements

This research was, in part, supported by a tar ball characterization and assessment grant funded by the Alabama Emergency Management Agency (AEMA 224637). Additional fellowship support for this research was provided by the Department of Civil Engineering at Auburn University and the Woltosz Fellowship. The authors would like to thank the following people for their contributions to this research: Pamela Turner at the National Center for Asphalt Technology for her assistance with viscosity measurements; Dr. Allan David and his research group in the Department of Chemical Engineering at Auburn University, particularly Prachi Sangle for her guidance and use of equipment for microscopic analysis; and Dr. Stephanie Shepherd for her assistance with characterizing the kaolinite used in this study. SAG conducted experimental work, developed ideas, wrote the manuscript, and revised the work; GFJ made suggestions for analytical work, performed asphaltene content analysis, and reviewed/revised the manuscript; and TPC supervised the work, provided the resources, helped develop the hypotheses and discussed ideas, and reviewed/revised the manuscript. Overall, all three authors have contributed to this effort and their relative responsibilities, estimated using the Clement (2014) approach, are: SAG (65%), GFJ (15%) and TPC (20%).

References

ASTM D3279-12, 2012. Standard Test Method for n-Heptane Insolubles. ASTM International.
Ajijolaiya, L.O., Hill, P.S., Khelifa, A., Islam, R.M., Lee, K., 2006. Laboratory investigation of the effects of mineral size and concentration on the formation of oil-mineral aggregates. Mar. Pollut. Bull. 52, 920–927.
Bobra, M., 1991. Water-in-oil emulsification: a physicochemical study. International Oil Spill Conference. American Petroleum Institute, pp. 483–488.
Bragg, J.R., Owens, E.H., 1995. Shoreline cleansing by interactions between oil and fine mineral particles. International Oil Spill Conference. American Petroleum Institute, pp. 219–227.
Bragg, J.R., Yang, S.H., 1995. Clay-oil flocculation and its role in natural cleansing in Prince William Sound following the Exxon Valdez oil spill. Exxon Valdez Oil Spill: Fate and Effects in Alaskan Waters. ASTM International.
Cai, Z., Fu, J., Liu, W., Fu, K., O'Reilly, S., Zhao, D., 2017. Effects of oil dispersants on settling of marine sediment particles and particle-facilitated distribution and transport of oil components. Mar. Pollut. Bull. 114, 408–418.
Chapman, H., Purnell, K., Law, R.J., Kirby, M.F., 2007. The use of chemical dispersants to combat oil spills at sea: a review of practice and research needs in Europe. Mar. Pollut. Bull. 54, 827–838.
Chen, L., Zhou, Y., Wang, X., Zwicker, T., Lu, J., 2013. Enhanced oil–mineral aggregation with modified bentonite. Water Sci. Technol. 67, 1581–1589.
Clement, T.P., 2014. Authorship matrix: a rational approach to quantify individual contributions and responsibilities in multi-author scientific articles. Sci. Eng. Ethics 20, 345–361.
Clement, T.P., John, G.F., Yin, F., 2017. Assessing the increase in background oil contamination levels in Alabama's nearshore beach environment resulting from the Deepwater Horizon oil spill. Oil Spill Science and Technology, second ed. Elsevier Publishers, pp. 851–888.
Delvigne, G.A.L., Sweeney, C.E., 1988. Natural dispersion of oil. Oil Chem. Pollut. 4, 281–310.
Fitzpatrick, F.A., Boufadel, M.C., Johnson, R., Lee, K.W., Graan, T.P., Bejarano, A.C., Zhu, Z., Waterman, D., Capone, D.M., Hayter, E., 2015. Oil-particle Interactions and Submergence From Crude Oil Spills in Marine and Freshwater Environments: Review of the Science and Future Research Needs. US Geological Survey.
Gong, Y., Zhao, X., Cai, Z.Q., O'Reilly, S.E., Hao, X., Zhao, D., 2014. A review of oil, dispersed oil and sediment interactions in the aquatic environment: influence on the fate, transport and remediation of oil spills. Mar. Pollut. Bull. 79, 16–33.
Guyomarch, J., Le Floch, S., Merlin, F., 2002. Effect of suspended mineral load, water salinity and oil type on the size of oil-mineral aggregates in the presence of chemical dispersant. Spill Sci. Technol. Bull. 8, 95–100.
Jernelöv, A., Lindén, O., 1981. Ixtoc I: a case study of the world's largest oil spill. Ambio 299–306.
John, G.F., Han, Y., Clement, T.P., 2016. Weathering patterns of polycyclic aromatic hydrocarbons contained in submerged Deepwater Horizon oil spill residues when re-exposed to sunlight. Sci. Total Environ. 573, 189–202.
Kepkay, P.E., Bugden, J.B.C., Lee, K., Stoffyn-Egli, P., 2002. Application of ultraviolet fluorescence spectroscopy to monitor oil-mineral aggregate formation. Spill Sci. Technol. Bull. 8, 101–108.
Khelifa, A., Fieldhouse, B., Wang, Z., Yang, C., Landriault, M., Fingas, M., Brown, C.E., Gamble, L., Pjontek, D., 2007. A laboratory study on formation of oil-SPM aggregates using the NIST standard reference material 1941b. Arctic and Marine Oil Spill Program Technical Seminar. Environment Canada 1999, p. 35.
Khelifa, A., Fingas, M., Brown, C., 2008. Effects of Dispersants on Oil-SPM Aggregation and Fate in US Coastal Waters. Final Report (Grant Number: NA04NOS4190063).
Khelifa, A., Stoffyn-Egli, P., Hill, P.S., Lee, K., 2002. Characteristics of oil droplets stabilized by mineral particles: effects of oil type and temperature. Spill Sci. Technol. Bull. 8, 19–30.
Kujawinski, E.B., Kido Soule, M.C., Valentine, D.L., Boysen, A.K., Longnecker, K., Redmond, M.C., 2011. Fate of dispersants associated with the Deepwater Horizon oil spill. Environ. Sci. Technol. 45, 1298–1306.
Lee, K., Li, Z., Robinson, B., Kepkay, P.E., Blouin, M., Doyon, B., 2011. Field trials of in-situ oil spill countermeasures in ice-infested waters. International Oil Spill Conference Proceedings (IOSC). American Petroleum Institute (p. abs160).
Lee, K., Lunel, T., Wood, P., Swannell, R., Stoffyn-Egli, P., 1997. Shoreline cleanup by acceleration of clay-oil flocculation processes. International Oil Spill Conference. American Petroleum Institute, pp. 235–240.
Lee, K., Stoffyn-Egli, P., Tremblay, G.H., Owens, E.H., Sergy, G.A., Guenette, C.C., Prince, R.C., 2003. Oil-mineral aggregate formation on oiled beaches: natural attenuation and sediment relocation. Spill Sci. Technol. Bull. 8, 285–296.
Lee, K., Stoffyn-Egli, P., Wood, P., Lunel, T., 1998. Formation and Structure of Oil-Mineral Fines Aggregates in Coastal Environments.
Lee, K., Weise, A.M., St-Pierre, S., 1996. Enhanced oil biodegradation with mineral fine interaction. Spill Sci. Technol. Bull. 3, 263–267.
Lee, K., Zheng, Y., Merlin, F.X., Li, Z., Niu, H., King, T., Robinson, B., Kepkay, P.E., Wohlgeschaffen, G.D., Doane, R., 2012. Combining Mineral Fines With Chemical Dispersants to Disperse Oil in Low Temperature and Low Mixing Environments, Including the Arctic. US Department of the Interior, Bureau of Safety and Environmental Enforcement (BSEE).
Lee, R.F., 2003. Photo-oxidation and photo-toxicity of crude and refined oils. Spill Sci. Technol. Bull. 8, 157–162.
Li, Z.K., Kepkay, P., Lee, K., King, T., Boufadel, M.C., Venosa, A.D., 2007. Effects of chemical dispersants and mineral fines on crude oil dispersion in a wave tank under breaking waves. Mar. Pollut. Bull. 54, 983–993.
Linden, O., 1975. Acute effects of oil and oil/dispersant mixture on larvae of Baltic herring. Ambio 130–133.
Ma, X., Cogswell, A., Li, Z., Lee, K., 2008. Particle size analysis of dispersed oil and oil-mineral aggregates with an automated ultraviolet epi-fluorescence microscopy system. Environ. Technol. 29, 739–748.
Niu, H., Li, Z., Lee, K., Kepkay, P., Mullin, J., 2010. A method for assessing environmental risks of oil-mineral-aggregate to benthic organisms. Hum. Ecol. Risk. Assess. 16, 762–782.
Omotoso, O.E., Munoz, V.A., Mikula, R.J., 2002. Mechanisms of crude oil–mineral interactions. Spill Sci. Technol. Bull. 8, 45–54.
Oudot, J., Merlin, F., Pinvidic, P., 1998. Weathering rates of oil components in a bioremediation experiment in estuarine sediments. Mar. Environ. Res. 45, 113–125.
Owens, E.H., Lee, K., 2003. Interaction of oil and mineral fines on shorelines: review and assessment. Mar. Pollut. Bull. 47, 397–405.
Owens, E.H., Michel, J., Davis Jr., R.A., Stritzke, K., 1995. Beach cleaning and the role of technical support in the 1993 Tampa Bay spill. International Oil Spill Conference. American Petroleum Institute, pp. 627–634.
Payne, J.R., Clayton, J.R., Kirstein, B.E., 2003. Oil/suspended particulate material interactions and sedimentation. Spill Sci. Technol. Bull. 8, 201–221.
Poirier, O.A., Thiel, G.A., 1941. Deposition of free oil by sediments settling in sea water. AAPG Bull. 25, 2170–2180.
Poteau, S., Argillier, J.-F., Langevin, D., Pincet, F., Perez, E., 2005. Influence of pH on stability and dynamic properties of asphaltenes and other amphiphilic molecules at the oil-water interface. Energy Fuel 19, 1337–1341.
Prince, R., Lessard, R., Clark, J., 2003. Bioremediation of marine oil spills. Oil Gas Sci. Technol. 58, 463–468.
Prince, R., Varadaraj, R., Fiocco, R., Lessard, R., 1999. Bioremediation as an oil spill response tool. Environ. Technol. 20, 891–896.
Ramachandran, S.D., Hodson, P.V., Khan, C.W., Lee, K., 2004. Oil dispersant increases PAH uptake by fish exposed to crude oil. Ecotoxicol. Environ. Saf. 59, 300–308.
Ramseur, J.L., 2010. Deepwater Horizon Oil Spill: The Fate of the Oil. Congressional Research Service, Library of Congress, Washington, DC.
Rasband, W.S., 2016. ImageJ. U.S. National Institutes of Health, Bethesda, Maryland, USA.
Silva, C.S., de Oliveira, O.M., Moreira, I.T., Queiroz, A.F., de Almeida, M., Silva, J.V., da Silva Andrade, I.O., 2015. Potential application of oil-suspended particulate matter aggregates (OSA) on the remediation of reflective beaches impacted by petroleum: a mesocosm simulation. Environ. Sci. Pollut. Res. 1–13.
Sørensen, L., Melbye, A.G., Booth, A.M., 2014. Oil droplet interaction with suspended sediment in the seawater column: influence of physical parameters and chemical dispersants. Mar. Pollut. Bull. 78, 146–152.
Stoffyn-Egli, P., Lee, K., 2002. Formation and characterization of oil-mineral aggregates. Spill Sci. Technol. Bull. 8, 31–44.
Sun, J., Khelifa, A., Zhao, C.C., Zhao, D.F., Wang, Z.D., 2014. Laboratory investigation of oil-suspended particulate matter aggregation under different mixing conditions. Sci. Total Environ. 473, 742–749.
Sun, J., Zheng, X.L., 2009. A review of oil-suspended particulate matter aggregation-a natural process of cleansing spilled oil in the aquatic environment. J. Environ. Monit. 11, 1801–1809.
Sun, J.A., Khelifa, A., Zheng, X.L., Wang, Z.D., So, L.L., Wong, S., Yang, C., Fieldhouse, B., 2010. A laboratory study on the kinetics of the formation of oil-suspended particulate matter aggregates using the NIST-1941b sediment. Mar. Pollut. Bull. 60, 1701–1707.
Trudel, K., Belore, R.C., Mullin, J.V., Guarino, A., 2010. Oil viscosity limitation on dispersibility of crude oil under simulated at-sea conditions in a large wave tank. Mar. Pollut. Bull. 60, 1606–1614.
Venosa, A.D., Holder, E.L., 2013. Determining the dispersibility of South Louisiana crude oil by eight oil dispersant products listed on the NCP Product Schedule. Mar. Pollut. Bull. 66, 73–77.

Venosa, A.D., King, D.W., Sorial, G.A., 2002. The baffled flask test for dispersant effectiveness: a round robin evaluation of reproducibility and repeatability. Spill Sci. Technol. Bull. 7, 299–308.
Wang, W., Zheng, Y., Lee, K., 2013. Chemical dispersion of oil with mineral fines in a low temperature environment. Mar. Pollut. Bull. 72, 205–212.
Wang, W.Z., Zheng, Y., Li, Z.K., Lee, K., 2011. PIV investigation of oil-mineral interaction for an oil spill application. Chem. Eng. J. 170, 241–249.
Weise, A., Nalewajko, C., Lee, K., 1999. Oil-mineral fine interactions facilitate oil biodegradation in seawater. Environ. Technol. 20, 811–824.
Wolfe, D.A., Hameedi, M., Galt, J., Watabayashi, G., Short, J., O'CLAIRE, C., Rice, S., Michel, J., Payne, J., Braddock, J., 1994. The fate of the oil spilled from the Exxon Valdez. Environ. Sci. Technol. 28, 560A–568A.
Yin, F., John, G.F., Hayworth, J.S., Clement, T.P., 2015. Long-term monitoring data to describe the fate of polycyclic aromatic hydrocarbons in Deepwater Horizon oil submerged off Alabama's beaches. Sci. Total Environ. 508, 46–56.
Zhang, H.P., Khatibi, M., Zheng, Y., Lee, K., Li, Z.K., Mullin, J.V., 2010. Investigation of OMA formation and the effect of minerals. Mar. Pollut. Bull. 60, 1433–1441.